

MIT Open Access Articles

*Modular synthesis of polymers containing
2,5-di(thiophenyl)- N-arylpyrrole*

The MIT Faculty has made this article openly available. **Please share**
how this access benefits you. Your story matters.

Citation: Truong, Tran N. B. et al. "Modular synthesis of polymers containing 2,5-di(thiophenyl)-N-arylpyrrole." *Journal of polymer science. Part A, Polymer chemistry* 56 (2018): 1133-1139 © 2018 The Author(s)

As Published: <https://dx.doi.org/10.1002/POLA.28990>

Publisher: Wiley

Persistent URL: <https://hdl.handle.net/1721.1/125533>

Version: Author's final manuscript: final author's manuscript post peer review, without publisher's formatting or copy editing

Terms of use: Creative Commons Attribution-Noncommercial-Share Alike





Published in final edited form as:

J Polym Sci A Polym Chem. 2018 June 1; 56(11): 1133–1139. doi:10.1002/pola.28990.

Modular Synthesis of Polymers Containing 2,5-di(thiophenyl)-N-arylpyrrole

Tran N. B. Truong¹, Suchol Savagatrup¹, Intak Jeon², and Timothy M. Swager¹

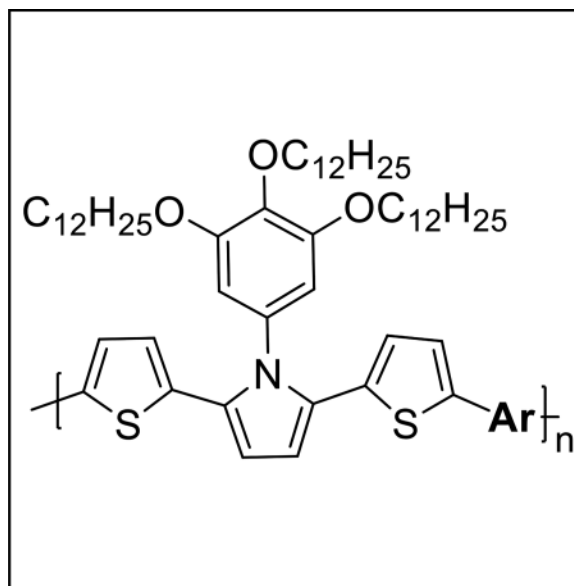
¹Department of Chemistry, Massachusetts Institute of Technology, Cambridge, MA 02139, USA

²Department of Materials Science and Engineering, Massachusetts Institute of Technology, Cambridge, MA 02139, USA

Abstract

A modular facile route has been developed to synthesize functionalized 2,5-di(thiophen-2-yl)-1-H-arylpyrroles from readily available starting materials. These units are compatible with various polymerization conditions and are versatile building blocks for conjugated polymers. The polymers show high thermal stability and solubility in a number of solvents. Characterization of the polymers reveals a correlation between molecular packing, controllable by polymer design, and charge carrier mobility.

Graphical Abstract



This paper presents a modular and facile route to synthesize 2,5-dithiophenyl-arylpyrrole analogs, versatile building blocks for conjugated polymers. This synthetic strategy enables easy

Correspondence to: Timothy M. Swager (tswager@mit.edu).

Additional Supporting Information may be found in the online version of this article.

customization of conjugated polymers for electronic applications. The polymers synthesized in this study exhibit high thermal stability and solubility in various solvents.

Keywords

conjugated polymers; co-polymer; Paal-Knorr pyrrole synthesis; 2,5-di(thiophen-2-yl)-1-H-arylpyrrole; organic electronics

INTRODUCTION

Conjugated polymer semiconductors afford many advantages over the inorganic counterparts such as the ability to be processed through roll-to-roll fabrication,¹ robust mechanical properties,² and tunability through molecular design and synthesis.³ The ability to tune various properties of conjugated polymers is critical to performance in specific applications, namely organic photovoltaic (OPV),⁴ organic light emitting diodes (OLED),^{5,6} and organic field-effect transistors (OFET).⁷ The customization and molecular engineering can, however, require extensive synthetic sequences that result in low yields and rely on environmentally unfriendly methods.^{8,9} Thus there is a strong need for simple, robust, and scalable routes to synthesize modular building blocks that can be readily incorporated into a variety of conjugated polymers.¹⁰

A common approach to fine-tune the physical properties of semiconducting polymers is to attach sidechains and functional groups to the polymer backbone. This approach can be performed via post-polymerization modifications or by polymerization of a functionalized monomer.¹¹ Alkylated polythiophenes are among the most popular semiconducting polymer building blocks; and, in cases with a single alkyl chain on each repeating unit, regioregularity is a major factor that affects polymers' solid-state structure and device performance.¹² Site-selective Grignard metathesis (GRIM) polymerization or direct arylation polymerization can provide regioselectivity up to 99.3% in the production of regioregular thiophenes.^{13,14} However, the issue of regioregularity can be avoided with the use of symmetrical monomers.

We have been interested in 2,5-dithiophenylpyrrole as a core building block to create an expanded family of polymers. Our interest is motivated by the fact that previous studies of 2,5-dithiophenylpyrrole-derived materials display similar conductivity to polymers containing *tert*-thiophenyl units, while providing an additional handle for functionalization of the pyrrole rings at the 3,4 and N-positions.¹⁵ N-functionalization is particularly attractive, as it can be done in a modular manner and retain the symmetry of the unit and regioregularity of the polymer, which in turn can influence polymer packing and performance in devices.¹⁶ McLeod et al. first accessed 2,5-dithiophenylpyrrole derivatives via the Paal-Knorr pyrrole synthesis using 1,4-dithienyl-butanone and methyl amine starting materials.¹⁷ This synthetic route generally involves double condensation reactions, using a catalytic amount of acid or an acidic solvent, which are not compatible with some functional groups. Further efforts have extended this method to attach different functional groups to the polymer backbone, including alkyl,¹⁸ phenyl,^{19–22} and pyridinyl groups.²³ Aryl rings can also be attached to the 2,5-dithiophenylpyrrole unit via a linker.^{24–26} We are especially

interested in the direct incorporation of N-aryl group, which allows for electronically coupled functionality that can introduce organization by increased π -stacking or enhance light absorption, both of which are of interest for the design of active materials in photovoltaic devices.¹⁹ Furthermore, the aryl groups incorporated via this route are capable of bearing solubilizing side chains without affecting the symmetry of the monomers.²⁵

Herein we explore a modular synthetic scheme to synthesize 2,5-di(thiophen-2-yl)-1-H-arylpyrroles as building blocks for conjugated polymers. The monomers are produced in modular and robust synthetic operations: attachment of alkoxy side chains onto an aryl ring followed by a modified Paal-Knorr reaction with a 1,4-diketone. By employing solubilizing side chains on the monomer, we were able to incorporate different types of co-monomers without the need for additional solubilizing side chains.

EXPERIMENTAL

General

The reagent-grade starting materials were obtained from commercial sources and used without further purification. For general experimental procedures and instrumentation, see Supporting Information.

Synthesis

Synthesis of Monomers

Synthesis of 3,4,5-tris(dodecyloxy)benzenaminium chloride salt (3): A suspension of **2** (6.1 g, 9 mmol) and tin(II) chloride dihydrate (8.4 g, 45 mmol) in ethanol (450 mL) and concentrated hydrochloric acid (180 mL) was refluxed for 16 h. The reaction mixture was cooled to room temperature and the white precipitate was collected by filtration, washed with concentrated hydrochloric acid (3 \times 15 mL), and dried in vacuum to give product **3** as a white solid (6.0 g, 98%). ¹H NMR (400 MHz, CDCl₃) δ 10.36 (bs, 3H), 6.70 (s, 2H), 3.95 (t, J = 6.4 Hz, 4H), 3.90 (t, J = 6.5 Hz, 2H), 1.75 (m, 8H), 1.52 – 0.97 (m, 52H), 0.88 (t, J = 6.6 Hz, 9H); ¹³C NMR (100 MHz, CDCl₃) δ 154.03, 138.35, 124.57, 101.54, 73.55, 69.41, 31.94, 30.28, 29.75, 29.72, 29.70, 29.68, 29.65, 29.61, 29.43, 29.40, 29.38, 29.26, 26.11, 22.70, 14.12. HRMS (ESI, m/z): [M - Cl]⁺ calcd for C₄₂H₈₀NO₃, 646.6133; found 646.6123.

Synthesis of 2,5-bis(5-bromothiophen-2-yl)-1-(3,4,5-tris(dodecyloxy)phenyl)-1H-pyrrole (5): Compounds **3** (1 mmol) and **4** (1 mmol) were dissolved in dry pyridine (5ml) under nitrogen. Trimethylsilyl chloride (5mmol) was added. The reaction was run on reflux for 16 hours. The solvent was removed in vacuo. The crude mixture was purified by flash column chromatography with hexanes: dichloromethane 1:9 as the eluent to give a light yellow solid (75% yield), m.p. 82.9°C; ¹H NMR (400 MHz, CDCl₃) δ 6.78 (d, J = 3.9 Hz, 2H), 6.48 (s, 2H), 6.46 (s, 2H), 6.42 (d, J = 3.9 Hz, 2H), 4.05 (t, J = 6.5 Hz, 2H), 3.87 (t, J = 6.6 Hz, 2H), 1.75 (m, 8H), 1.52 – 0.97 (m, 52H), 0.88 (t, J = 6.6 Hz, 9H); ¹³C NMR (100 MHz, CDCl₃) δ 153.45, 139.33, 136.12, 132.28, 129.73, 129.71, 124.07, 110.68, 109.40, 108.63, 73.66, 69.33, 31.96, 31.94, 30.24, 29.78, 29.76, 29.72, 29.70, 29.67, 29.63, 29.41,

29.38, 29.10, 26.13, 25.97, 22.70, 14.13. HRMS (ESI, m/z): $[M + H]^+$ calcd for $C_{54}H_{83}Br_2NO_3S_2$, 1018.4252; found 1018.4250.

Synthesis of Polymers

General synthesis of polymers via Stille polycondensation reaction (P1, P2, P3): Monomer **5** (1 equiv.), the bis(trimethylstannyl) aryl co-monomer (1 equiv.), tris(dibenzylideneacetone)dipalladium(0) (0.05 equiv.) and tri(*o*-tolyl)phosphine (0.2 equiv.) were dissolved in dry toluene. The mixture was degassed via 3 freeze-pump-thaw cycles and then stirred at 100°C for 24 hours. The reaction was quenched with concentrated potassium fluoride solution. The reaction mixture was added dropwise into methanol under vigorous stirring. The residue was collected by filtration and washed with methanol, acetone and hexanes. More details can be found in the Supporting Information.

Synthesis of Polymer P4 via Suzuki-Miyura polycondensation reaction: To a dry Schlenk flask equipped with a magnetic stir bar was added monomer **5** (204 mg, 0.2 mmol, 1 equiv.) and 4,7-bis(4,4,5,5-tetramethyl-1,3,2-dioxaborolan-2-yl)benzo[c][1,2,5]thiadiazole (78 mg, 1 equiv.). To this mixture was added 2 ml of toluene, a drop of Aliquat 336 and 20 equiv. of Na_2CO_3 in 2M aqueous solution. The mixture was then degassed via 3 freeze-pump-thaw cycles, and 4 mol % of Pd_2dba_3 and 32 mol % of $P(o\text{-tolyl})_3$ were added against a flow of argon. The mixture was stirred at 105°C for 24 hours. The reaction mixture was then diluted with chloroform, precipitated in methanol and filtered. The residue was washed with methanol, acetone and hexanes to give a purple solid product (70% yield, m.p. 197.3°C, molecular weight M_n 7 kg/mol (GPC), UV-vis (chloroform): $\lambda_{max} = 606$ nm).

Synthesis of Polymer P5 via Nickel-catalyzed Grignard Metathesis (GRIM) polymerization reaction: $iPrMgCl \cdot LiCl$ (1 equiv.) was added dropwise to a solution of **5** in dry tetrahydrofuran at 0°C. The solution was stirred at room temperature for 2 hours. $Ni(dppe)Cl_2$ was then added. The resulting solution was stirred at room temperature for 24 hours. The reaction was quenched with concentrated potassium fluoride solution. The reaction mixture was added dropwise to a mixture of methanol and 1M HCl. The bright orange oligomer collected is highly soluble in common organic solvents (70% yield, m.p. 149.3°C, molecular weight 8.6 kg/mol (GPC), UV-vis (chloroform): $\lambda_{max} = 473$ nm).

RESULTS AND DISCUSSION

Synthesis of Materials

Synthesis of Monomers—Monomers were synthesized in a modular fashion via the Paal-Knorr pyrrole synthesis as outlined in SCHEME 1. The 1,4-diketone component **4** was synthesized according to a literature procedure.²⁷ Based on modified literature procedures, the aniline component **3** is produced in three simple steps. First, pyrogallol was alkylated via a nucleophilic substitution reaction with the respective bromoalkane under basic conditions to give **1**.²⁸ This method is useful for attaching a variety of side chains to the respective phenol, enabling customization of the monomer in a modular manner. Compound **1** undergoes facile nitration to afford the nitro compound **2** by stirring with silica gel that has been previously treated with concentrated nitric acid.^{29,30} Reduction with tin (II) chloride

under acidic condition gives the anilinium salt in high yields. The isolation of **3** as a salt is important as the free base form of this molecule is mildly air-sensitive. These reduction conditions provide higher yield and more stable products than those in neutral conditions with hydrogen and palladium on activated carbon or hydrazine. The need for reduction under acidic conditions is most pronounced on substrates with multiple electron-donating groups such as **3**.

Condensation of compound **3** ($R = C_{12}H_{25}$) with **4** provides pyrrole-containing monomer **5**. Previously reported examples of similar Paal-Knorr pyrrole synthesis employ acidic conditions, with a catalytic amount of acid or with an acid as a co-solvent.^{15,19,27} An extensive survey by Lacaze and co-workers showed that although an acid is required to activate the diketone, an excess of acid might lead to formation of side products and decomposition of the main product.³¹ We found that acidic conditions afforded some product with our alkoxy anilines; however the yields of about 20% were unacceptably low. It is likely that the low yields are the result of decomposition of the electron-rich aniline substrate as well as hydrolysis of the ether linkages with the acidic conditions. To alleviate this problem, we developed a procedure using pyridine as a solvent and trimethylsilyl chloride as a dehydrating agent. Under this new condition, the anilinium salt is activated *in situ* and affords higher yields in the condensation reaction, 65 – 80%. Pyridine also captures the hydrochloric acid generated and prevents hydrolysis of the ether linkages.

Synthetic SCHEME 1 provides access to 2,5-di(thiophen-2-yl)-1-H-arylpyrrole with a variety of side chains and function groups as shown in FIGURE 1. The milder non-acidic condensation conditions are critical for the derivatives containing polyethylene glycol as a side chain, which opens up a possibility of synthesizing conducting polymers that are water-soluble. It is also worth noting that SCHEME 1 quickly converts inexpensive starting materials into the desired conjugated polymers via a set of modular, robust reactions, and simple purification steps, mainly via recrystallization. Hence, this method constitutes a scalable, economical, and environmentally friendly synthesis of conjugated polymers.⁹

Synthesis of Polymers—Cross-coupling polymerization of monomer **5** was explored using Stille, Suzuki-Myura, and nickel-catalyzed Grignard metathesis (GRIM) reactions, as shown in SCHEME 2. Polymers **P1**, **P2**, and **P3** were synthesized via Stille polycondensation reaction and displayed molecular weights 13–22 kDa. Polymers **P4** and **P5** were synthesized by Suzuki-Miyura and Grignard metathesis (GRIM) polymerization reactions, respectively with somewhat lower molecular weights. This flexibility in the choice of polymerization method facilitates the future construction of polymer libraries based on commercially available co-monomers with different functional groups and chemical compatibilities. The resulting polymers are soluble in dichloromethane, chloroform, tetrahydrofuran, and dichlorobenzene. We observed that the polymers tend to assemble in aggregates at room temperature and break up upon heating. This feature is reflected in additional shoulder peaks in UV-Vis absorption spectra (FIGURE 2) as well as Gel Permeation Chromatograms (GPC) (Figure S15, Supporting Information). To prevent this aggregation, we measured the molecular weights of the polymers using a heated GPC column at 60°C in chlorobenzene. In these studies, we were not able to maintain heating at the injection point and upstream of the columns. It is possible that polymers with higher

molecular weight may have been aggregated and eliminated upstream of the heated columns, leading to an underestimation of the bulk molecular weights (TABLE 1).

Optical properties

FIGURE 2 shows the UV-visible absorption spectra of monomer **5** and the polymers containing **5** in chloroform solutions. The polymer absorption peaks are substantially red-shifted relative to **5** ($\lambda_{\text{max}} = 340$ nm). Polymers **P1**, **P2**, and **P3** have similar absorption spectra, with absorption peaks from 526 to 536 nm and a low-energy shoulder peak caused by aggregation of the polymer chains in solution. This lower energy absorption is caused by aggregation-induced planarization of the polymer backbones and potentially π -stacking interactions. The shoulder peak is the most prominent in **P1**, suggesting that a higher density of alkoxy groups leads to an increase in polymer chain aggregation.

From FIGURE 2, polymer **P3** absorbs at a slightly shorter wavelength than **P1** and **P2**. The integration of thieno[3,2-*b*]thiophene to polymer backbones has been known to have diverse effects on the electronics of the polymers.^{32,33} In this case, a possible explanation is that the delocalization of electrons from this fused aromatic unit into the backbone is less favorable than from a single thiophene ring, due to the larger resonance stabilization energy of the fused ring over the single thiophene ring.³³ This reduced delocalization along the backbone results in a lowering of the polymer highest occupied molecular orbital level and thus increasing the bandgap, resulting in a more blue-shifted absorption of **P3**.

In addition to the π - π^* transition peak at around 405 nm, polymer **P4** also has a low-energy peak which could be attributed to the internal charge transfer between the donor and acceptor units. This peak with the onset at 750 nm corresponds to a low bandgap of 1.65 eV. These types of low-bandgap polymers are especially useful in photovoltaic applications.³⁴

FIGURE 3 shows the comparative absorption spectra of the polymers in solution vs. the thin film. The absorption spectra of **P1**, **P2**, and **P3** films were very similar to those of the corresponding solutions, whereas for polymers **P4** and **P5**, we observed a more significant red shift in the solid state. This smaller red shifts for **P1–P3** polymer chains may be related to their greater tendency to aggregate in solution, possibly as a result of their higher molecular weights.

Electrochemical properties

The redox properties of the polymers were studied via cyclic voltammetry. The measurements were performed on polymer films with 0.1 M TBAPF₆/acetonitrile as the electrolyte. The results are summarized in FIGURE 4. The highest occupied molecular orbital (HOMO) was calculated based on the formula $\text{HOMO} = -(4.8 + E^{\text{ox}})$ eV, where E^{ox} was the oxidation potential relative to ferrocene.

All the polymers showed a reversible oxidation peak at 0.2–0.34 V relative to ferrocene, corresponding to HOMO levels of -5.06 – -5.12 eV. The reversibility and Coulombic efficiency of the voltammograms indicate that the polymers are stable in their oxidized states. The polymers have lower oxidation potential than polythiophene and are comparable to other dithiophenylpyrrole polymers.^{15,17,20} **P3** has the lowest oxidation potential of the

polymers investigated, which likely reflects the presence of electron-rich thieno[3,2-*b*]thiophene groups in the backbone.

Thermal properties

Thermal gravimetric analysis (TGA) (FIGURE 5) indicates that most of the polymers have high decomposition temperatures at above 400°C. The homopolymer **P5** has the lowest decomposition temperature at 300°C. Differential scanning calorimetry results (DSC) as represented by **P2** (FIGURE 6) revealed that most of the polymers have similar melting points of about 200°C. Polymer **P2** showed the most prominent glass transition peak, followed by **P1** and **P3**. Homopolymer **P5** has the lowest melting point and no observable glass transition peak. This result suggests that the high density of alkyl chains reduces crystallinity in the polymers. The high thermal stability and lower melting temperatures of these materials present opportunities to create melt-processed devices, reducing the need for solvent processing.³⁵

X-ray Diffraction Studies

The solid-state organization of the polymers was investigated by X-ray diffraction (XRD). The polymers were dropcast onto silicon substrates and annealed above their glass transition temperatures (150°C) to produce XRD diffraction peaks with the highest intensity.

The XRD diffractograms (Figure S19, Supporting Information) give diffraction patterns with 3 peaks, suggestive of a lamellar structure, similar to that of poly(3-alkylthiophene)s. All the polymers share a common peak with $2\theta = 20^\circ$, corresponding to a d-spacing of 4.5 Å, as commonly observed for π - π stacking of aromatic polymer backbones.³⁶ These peaks are relatively broad and hence the regularity of the lateral interchain associations appears to be less than usually observed. Additionally, we observe considerable diffuse scattering from the disordered alkyl sidechains that are convolved with these signals. We also observed small peaks centered about 1.2 nm, which in some cases are at the proper location to be a second-order diffraction from the lamellar structure (*vide infra*). However, we cannot eliminate the possibility that there may be other interchain correlations with this periodic spacing. The most prominent peaks are at low angle and are consistent with what is usually associated with a lamellar periodic pattern driven by side-chain/main-chain segregation.³⁷ These d-spacing distances range from 2.6–2.7 nm (TABLE 2). Among these side-stacking peaks, **P2** has the sharpest XRD peak and the shortest d-spacing distance, followed by **P3** and **P1**. It appears that the greater spacing between alkyl chains in **P2** results in a more regular packing. This trend is in agreement with the thermal behaviors of the polymers as seen in the DSC results. Both the thermal and XRD results suggest that **P2** has the highest crystallinity, followed by **P3** and **P1**. The lack of a melting transition peak and any clear XRD peaks implies that **P5** is amorphous. The trends suggest that the extended spacing between the adjacent dithiophenylpyrrole units is necessary for efficient interdigitation of the alkoxy groups and stacking of the polymer chains.

Charge Mobility in Organic Field-Effect Transistors

Charge-transport properties of conjugated polymers are generally highly dependent on the degree of interchain interaction in polymer thin films. Hole mobilities have been correlated

to the strength of aggregation as observed spectroscopically or by X-ray diffraction. To compare the hole mobilities of the polymer in this study, we fabricated bottom-gate, bottom-contact thin-film transistors (Figure S20, Supporting information).

The hole mobilities of the polymer films are summarized in TABLE 2. The mobilities of these polymers are lower than that of polythiophene, but comparable to other polymers containing 2,5-di(thiophen-2-yl)-1-H-arylpyrrole.^{15,38} The trends in the mobilities are consistent with the XRD data. Polymers with shorter d-spacing and more pronounced diffraction peaks afforded higher mobility. We attributed this effect to the stronger interchain interactions as a result of better interdigitation due to the alkoxy chains.¹¹ In future studies, it is possible that shorter alkoxy chains will further improve charge mobility while maintaining polymer solubility.³⁹

CONCLUSIONS

We have developed a facile, modular, and convergent synthetic route to synthesize 2,5-di(thiophen-2-yl)-1-H-arylpyrroles from simple starting materials and robust reactions. The monomers were compatible with different polymerization methods and are flexible building blocks for semiconducting polymers. The polymers exhibit high solubility and thermal stability, facilitating device fabrication. The characterization of the polymers suggests that changing the spacing of the sidechain-containing arylpyrroles can have a significant influence on the thermal properties, molecular packing, and charge carrier mobility of conjugated polymers. The general convergent synthetic scheme demonstrated access to a diversity via co-monomers and the functionalization of the aniline component. It is also possible to introduce functionality through the diketone component and hence access to an expanded scope of materials is also possible.²⁷

Supplementary Material

Refer to Web version on PubMed Central for supplementary material.

Acknowledgments

This work was sponsored by Eni S.p.A. as part of the efforts of the MIT-Eni Solar Frontiers Alliance. T.N.B.T acknowledges the support of the Agency of Science, Technology and Research (A*STAR), Singapore for the graduate fellowship. S.S. was supported by an F32 Ruth L. Kirschstein National Research Service Award.

REFERENCES AND NOTES

1. Krebs FC, Espinosa N, Hösel M, Søndergaard RR, Jørgensen M. *Adv. Mater.* 2014; 26:29–39. [PubMed: 24741693]
2. Root SE, Savagatrup S, Printz AD, Rodriguez D, Lipomi DJ. *Chem. Rev.* 2017; 117:6467–6499. [PubMed: 28343389]
3. Guo X, Baumgarten M, Müllen K. *Prog. Polym. Sci.* 2013; 38:1832–1908.
4. Dou L, You J, Hong Z, Xu Z, Li G, Street RA, Yang Y. *Adv. Mater.* 2013
5. Greenham NC, Moratti SC, Bradley DDC, Friend RH, Holmes AB. *Nature.* 1993; 365:628–630.
6. Pei Q, Yu G, Zhang C, Yang Y, Heeger AJ. *Science* (80-). 1995:269.
7. Sirringhaus H. *Adv. Mater.* 2014; 26:1319–1335. [PubMed: 24443057]
8. Burke DJ, Lipomi DJ. *Energy Environ. Sci.* 2013; 6:2053.

9. Po R, Bianchi G, Carbonera C, Pellegrino A. *Macromolecules*. 2015; 48:453–461.
10. Mcdearmon B, Lim E, O'Hara K, Nakayama H, Luo Y, Chabinyc ML, Hawker CJ, O'hara K, Nakayama H, Luo Y, Chabinyc ML, Hawker CJ. *J. Polym. Sci. Part A Polym. Chem.* 2017; 55:2618–2628.
11. Mei J, Bao Z. *Chem. Mater.* 2014; 26:604–615.
12. McCullough RD, Lowe RD, Jayaraman M, Anderson DL. *J. Org. Chem.* 1993; 58:904–912.
13. Osaka I, McCullough RD. *Acc. Chem. Res.* 2008; 41:1202–14. [PubMed: 18729480]
14. Pouliot J, Wakioka M, Ozawa F, Li Y, Leclerc M. *Macromol. Chem. Phys.* 2016; 217:1493–1500.
15. Pandule S, Oprea A, Barsan N, Weimar U, Persaud K. *Synth. Met.* 2014; 196:158–165.
16. McCullough RD, Lowe RD. *J. Chem. Soc. Chem. Commun.* 1992:70–72.
17. McLeod GG, Mahboubian-Jones MGB, Pethrick RA, Watson SD, Truong ND, Galin JC, François J. *Polymer*. 1986; 27:455–458.
18. Ferraris JP, Skiles GD. *Polymer*. 1987; 28:179–182.
19. Tamilavan V, Sakthivel P, Li Y, Song M, Kim C-H, Jin S-H, Hyun MH. *J. Polym. Sci. Part A Polym. Chem.* 2010; 48:3169–3177.
20. Kim YH, Hwang J, Son JI, Shim Y-B. *Synth. Met.* 2010; 160:413–418.
21. Soylemez S, Yılmaz T, Buber E, Udum YA, Özçubukçu S, Toppare L. *J. Mater. Chem. B*. 2017; 5:7384–7392.
22. Tirke S, Mersini J, Özta Z, Algi MP, Algi F, Cihaner A. *Electrochim. Acta*. 2013; 90:295–301.
23. Hwang J, Son JI, Shim Y-B. *Sol. Energy Mater. Sol. Cells*. 2010; 94:1286–1292.
24. Soganci T, Soyleyici HC, Giziroglu E, Ak M. *J. Electrochem. Soc.* 2016; 163:1096–1103.
25. Soganci T, Soyleyici HC, Ak M. *Phys. Chem. Chem. Phys.* 2016; 18:14401–14407. [PubMed: 27171850]
26. Yi it D, Hacio lu O, Güllü M, Toppare L. *New J. Chem.* 2015; 39:3371–3379.
27. Agneeswari R, Roh KH, Tamilavan V, Lee DY, Cho S, Jin Y, Park SH, Hyun MH. *Polym. Bull.* 2015; 72:1899–1919.
28. Yelamaggad Channabasaveshwar V, Achalkumar Ammathnadu S, Rao S ShankarPrasad SK. 2007
29. Seo S, Park J, Chang J. *Langmuir*. 2009; 25:8439–8441. [PubMed: 19284768]
30. Miłczak T, Jacniacki J, Zawadzki J, Malesa M, Skupi ski W. *Synth. Commun.* 2001; 31:173–187.
31. Just P, Chane-Ching K, Lacaze P. *Tetrahedron*. 2002; 58:3467–3472.
32. Li Y, Wu Y, Liu P, Birau M, Pan H, Ong BS. *Adv. Mater.* 2006; 18:3029–3032.
33. McCulloch I, Heeney M, Bailey C, Genevicius K, MacDonald I, Shkunov M, Sparrowe D, Tierney S, Wagner R, Zhang W, Chabinyc ML, Kline RJ, McGehee MD, Toney MF. *Nat. Mater.* 2006; 5:328–333. [PubMed: 16547518]
34. Bundgaard E, Krebs F. *Sol. Energy Mater. Sol. Cells*. 2007; 91:954–985.
35. Zhao Y, Zhao X, Roders M, Gumyusenge A, Ayzner AL, Mei J. *Adv. Mater.* 2016:1605056.
36. Friedel B, McNeill CR, Greenham NC. *Chem. Mater.* 2010; 22:3389–3398.
37. Roy I, Hazra S. *RSC Adv.* 2015; 5:665–675.
38. Erb T, Raleva S, Zhokhavets U, Gobsch G, Stuhn B, Spode M, Ambacher O. *Thin Solid Films*. 2004; 450:97–100.
39. Park YD, Kim H, Jang Y, Cho JH, Hwang M, Lee HS, Lim JA, Cho K. 2006

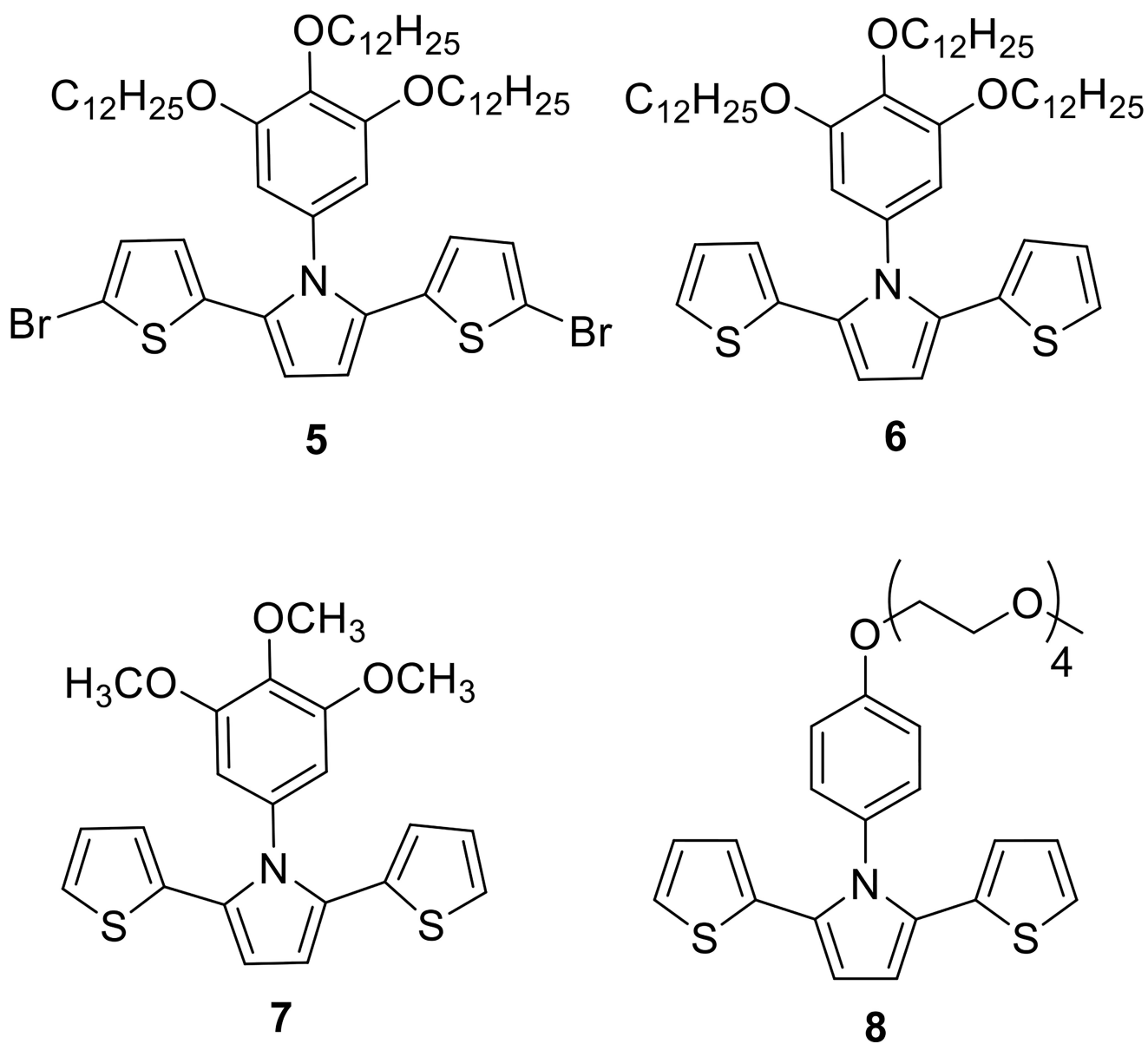


FIGURE 1.
Chemical structures of 2,5-di(thiophen-2-yl)-1-H-arylpyrrole with a variety of side chains and functional groups.

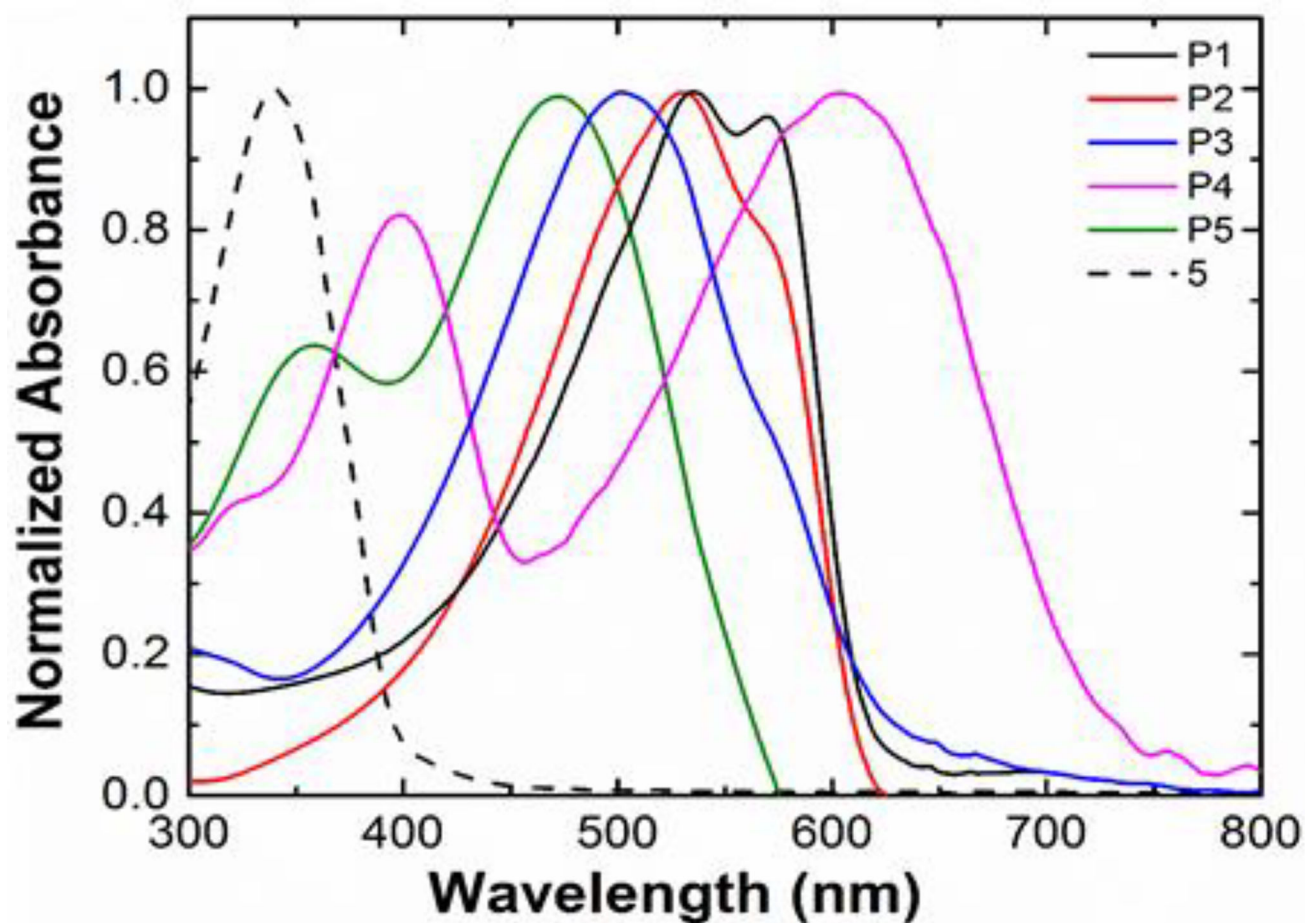


FIGURE 2.

UV-Vis absorption spectra of monomer **5** and polymers in chloroform solutions

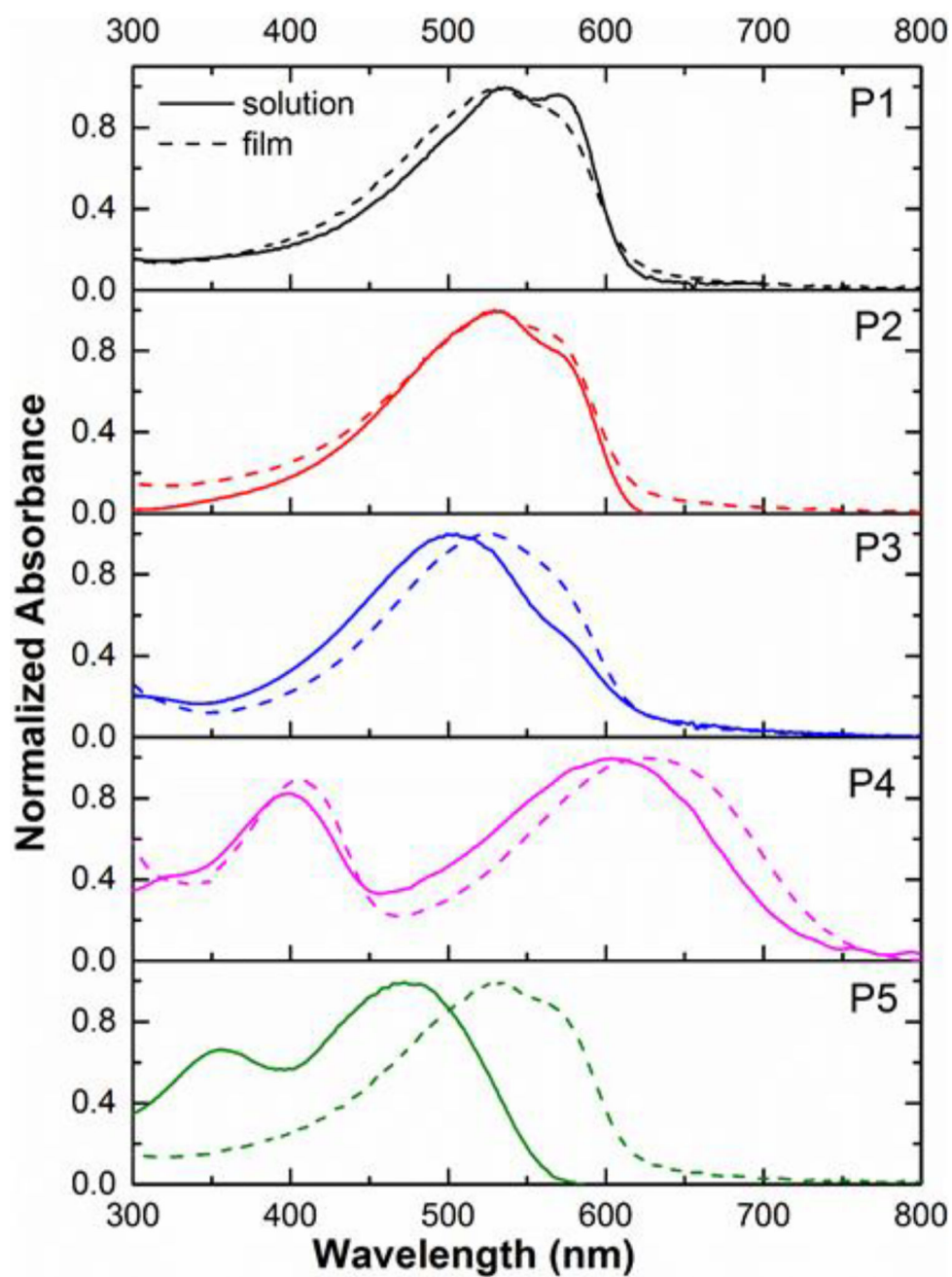


FIGURE 3. Absorption spectra of polymer chloroform solutions (solid) and spin-coated thin films on glass substrates (dashed)

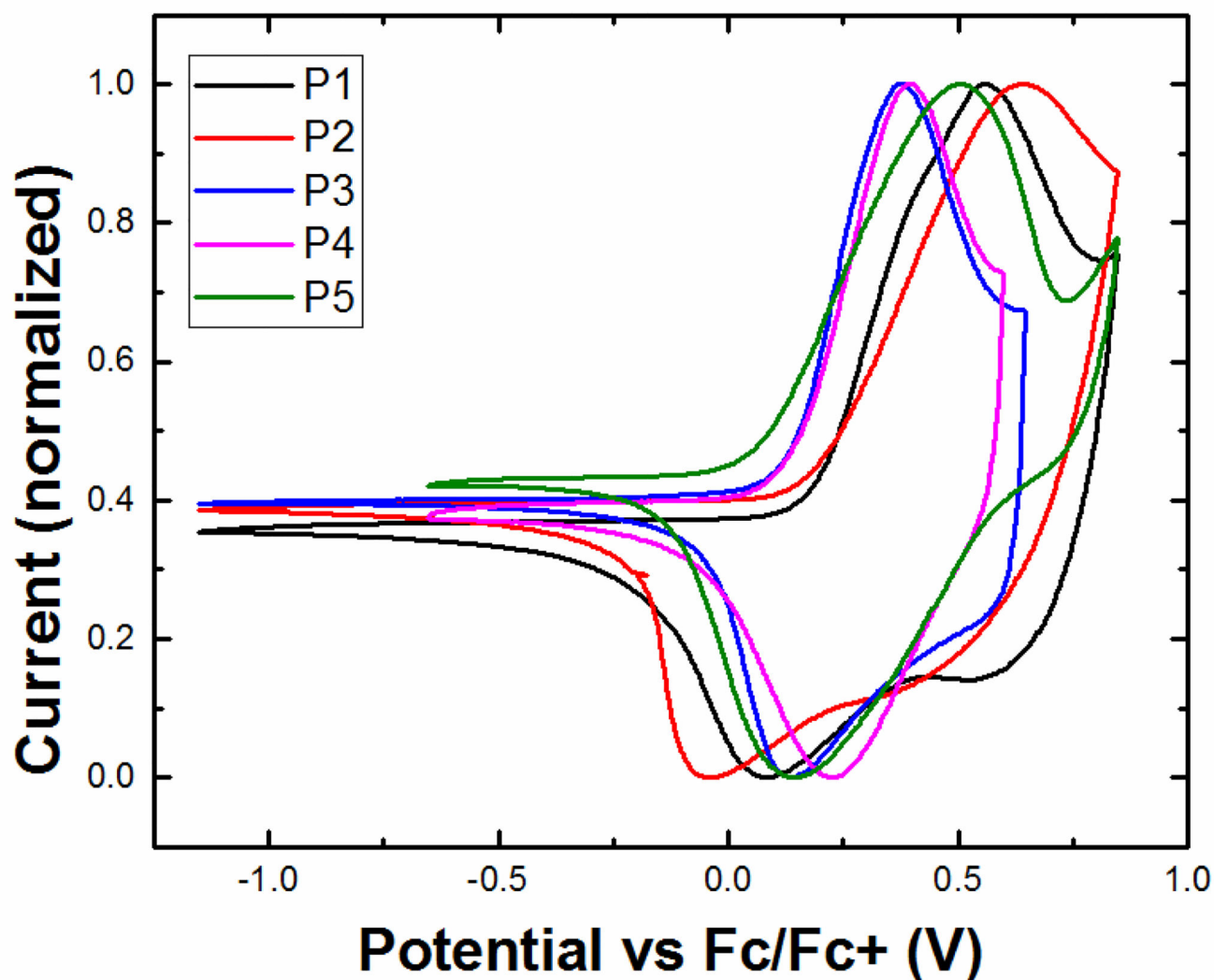


FIGURE 4.
Cyclic Voltammograms of Polymer Films Dropcast on ITO-coated glass substrates with 0.1M $n\text{-Bu}_4\text{PF}_6$ in acetonitrile as the electrolyte, scan rate 100 mV/s.

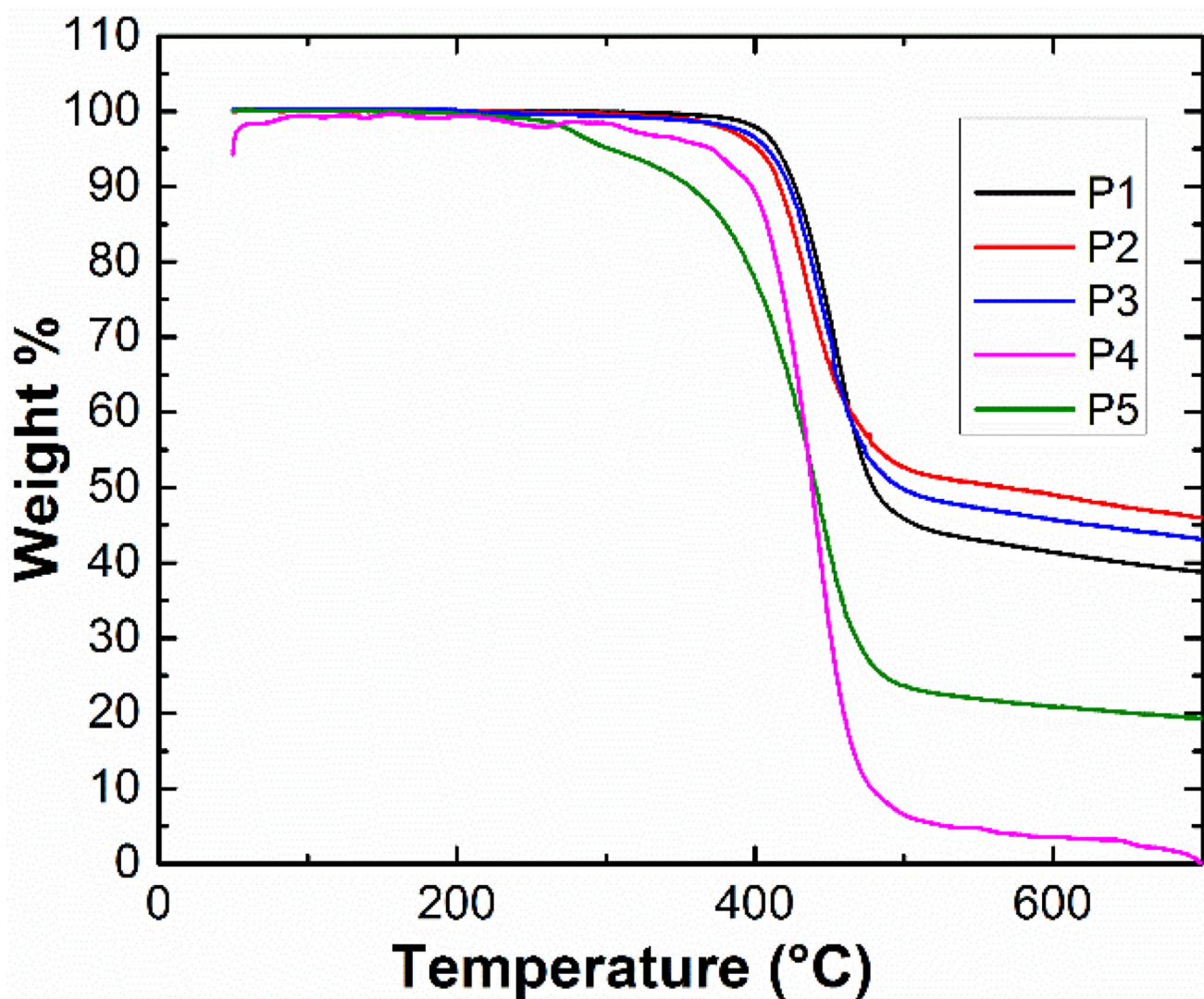


FIGURE 5.
Thermogravimetric Analysis (TGA) results of polymers, from 50°C to 700°C, scan rate
10 °C/min

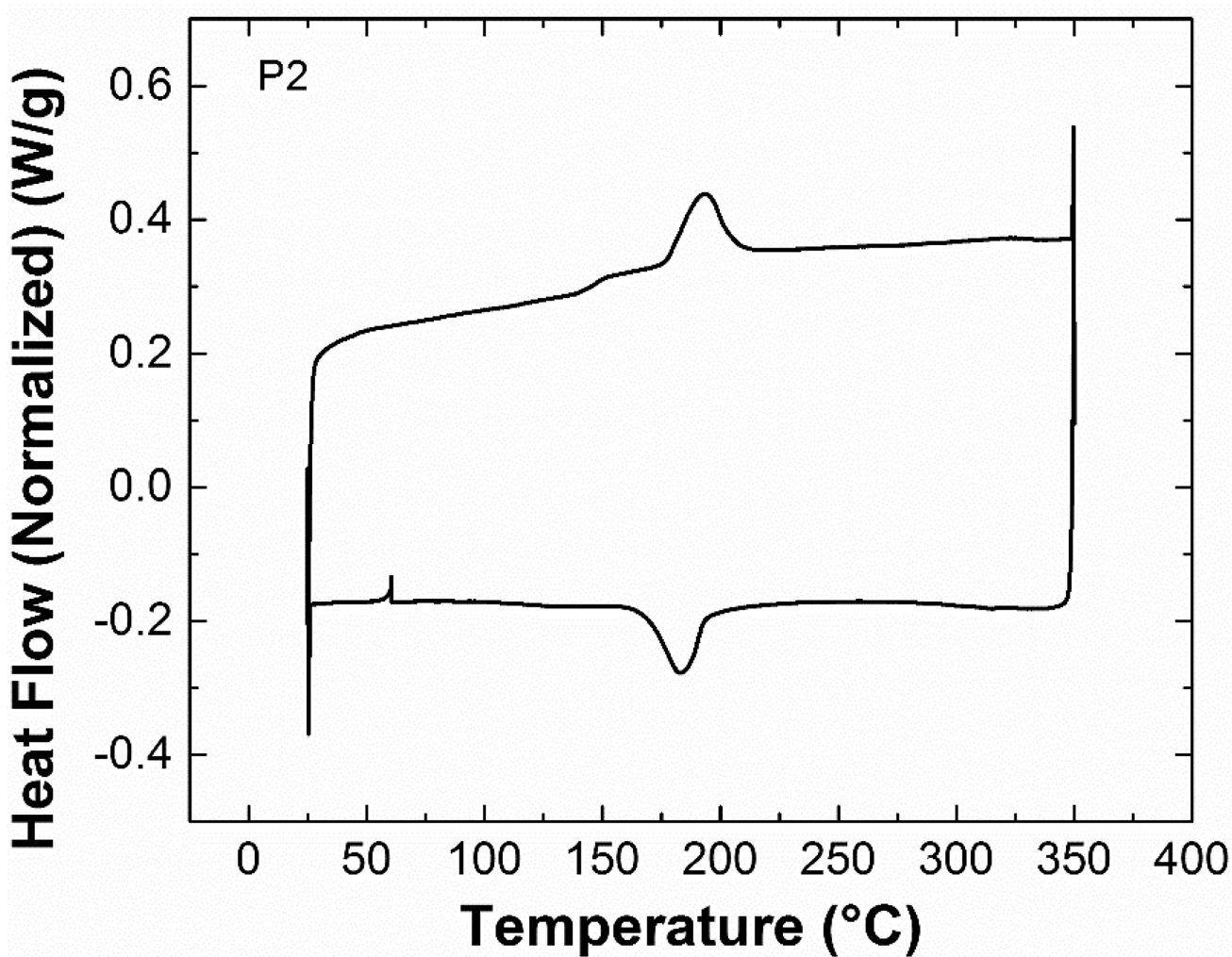
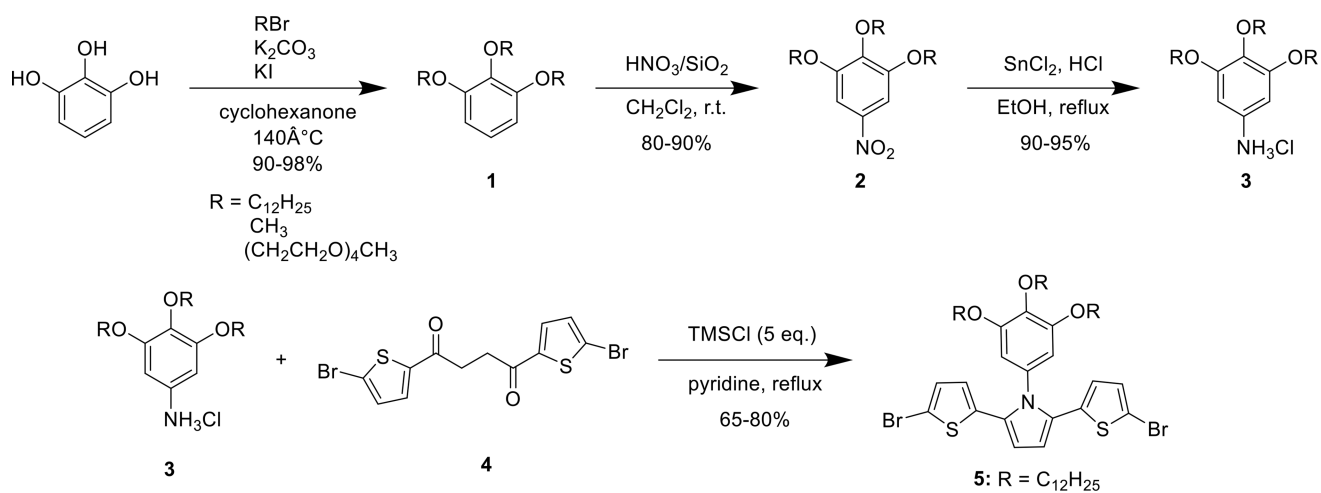
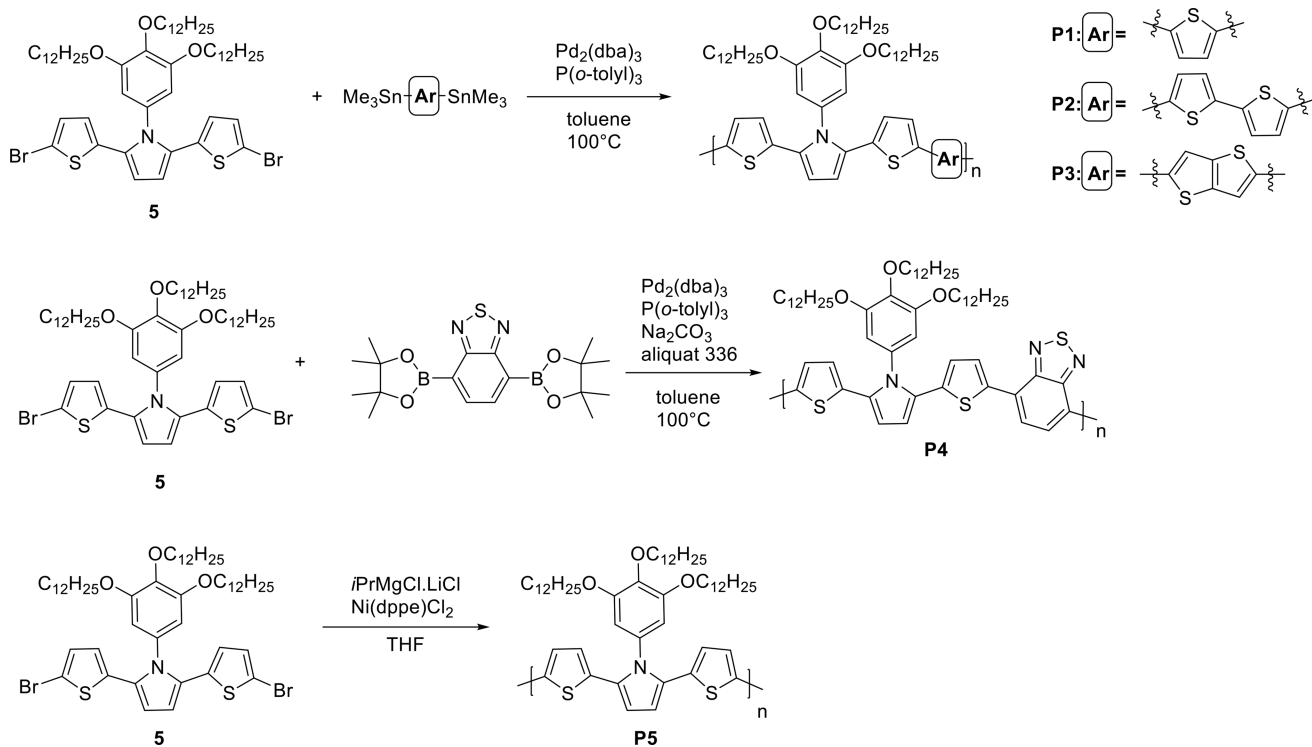


FIGURE 6.
Representative Differential Scanning Calorimetry (DSC) thermogram for **P2**, from 25 to 350°C, scan rate 10°C/min



SCHEME 1.
Synthesis of Monomers



SCHEME 2.
Polymer Synthesis from Monomer 5

TABLE 1
Polymerization method, molecular weight distribution, photophysical, and electrical properties of polymers

Polymer	Method	$M_n(kDa)^a$ /D	$\lambda_{max}^{(s)b}$ (nm)	$\lambda_{max}^{(f)b}$ (nm)	$\lambda_{onset}^{(f)}$ (nm)	$E_g^{opt}c$ (eV)	$E^{ox}d$ (eV)	HOMO ^e	LUMO ^f
P1	Stille	22/1.9	530	536	620	2.00	0.32	-5.12	-3.12
P2	Stille	13/1.8	526	529	618	2.00	0.34	-5.14	-3.14
P3	Stille	15/1.8	505	526	615	2.02	0.26	-5.06	-3.04
P4	Suzuki	7/2.9	606	627	750	1.65	0.31	-5.11	-3.46
P5	GRIM	8.6/1.6	473	530	610	2.03	0.32	-5.12	-3.09

^a Molecular weights were measured relative to polystyrene standard in heated column at 60°C

^b (s) and (f) refer to solution and film

^c The optical bandgap E_g^{opt} was estimated from the onset of the absorption of thin film

^d E^{ox} was estimated from cyclic voltammetry of the polymer film

^e HOMO was calculated according to the formula: $E_{HOMO} = -(E^{ox} + 4.8)(eV)$

^f LUMO was calculated as $HOMO + E_g^{opt}$

TABLE 2

D-spacing distance obtained from XRD and hole mobility from OFET (N = 4).

Polymer	d-spacing (nm)	μ ($10^{-3}\text{cm}^2\text{V}^{-1}\text{s}^{-1}$)
P1	2.68	0.021 ± 0.002
P2	2.58	0.031 ± 0.003
P3	2.66	0.013 ± 0.001